ENGINEERING RESEARCH JOURNAL (ERJ)
Vol. 1, No. 44 April 2020, pp.49-58.
Journal Homepage: erj.bu.edu.eg

Performance Characteristics of Pleated Air Filter Associated with Internal Combustion Engine

S. Allam[1], Ashraf Mimi Elsaid[2] and Ibrahim Shamsia[3]

1 Department of Vehicles and Tractors Technology, Faculty of Industrial Education, Helwan University.
2 Department of Refrigeration and Air-Conditioning Technology, Faculty of Industrial Education, Helwan University, 11282 Cairo, Egypt.
3 Department of Mechanical Power, Faculty of Industrial Education, Sohag University, Sohag, Egypt.

Abstract. This paper experimentally and numerically addressed the performance characteristics of pleated air filter with different parameters. The main objective is to enhance the I.C engine performance. The studied parameters are; pleat height, pleat spacing, media thickness, air velocity, and consume fuel. Experiments are done with air velocity from 1 to 5 m/s whereas the fuel volume was constant at $25x10^{-6}$ liter. Three different types of filters are explored as; loaded filter, standard filter, and optimized filter. Modeling of pleated air filter is designed using FLUENT 14.5 code. Filter media is developed as a porous zone. The results revealed that; the optimized pleated air filter provides a lower fuel consumption rate in comparing with standard filter and loaded filters.

Keywords: Pleat; filter; Diesel engine; Pressure drop.

Nomenclature

Symbol	Description
BP	Brake Power (kW)
B.S.F.C.	Brake fuel consumption, (kg/kW.hr)
C	Inertial factor of medium filter
H	Pleat height, (m)
K	Permeability factor of the medium filter
k	Thermal conductivity ($Wm^{-1}K^{-1}$)
L	Pleat length, (m)
$\dot{m}_f$	Fuel mass flow rate (kgs^{-1})
n	Engine rotational speed (rpm)
Pr	Prandtl number, (-)
T	Torque (Nm)
t	Thickness, (m)
u	Velocity vector, ($u_i + v_j$)
V	Fuel volume (m^3)
v	Average velocity (ms^{-1})

Greeks	
ρ	density (kgm^{-3})
ε	effectiveness
μ	viscosity ($kgm^{-1}s^{-1}$)
Abbreviations	
CFD	Computational fluid dynamics
I.C	Internal Combustion

1. INTRODUCTION

The filtration process is important in many applications [1] such as the automotive engine, passenger cabin, exhaust emission, and air conditioning applications, etc. The most traditional filter type which used in these applications is the pleated air filter to remove the impurities and minerals. The pleated air filter is composed of fibrous panels that reserve particulates such as dust, mold, and bacteria in airflow. In automotive applications, the air filter must supply the engine by a clean air with low-pressure drop. The air filter performs the separation process of the dust and particles from the air with less resistance to the flow. Due to the importance of the filter and the problems arise due to the lack filter where the air cannot mix the fuel used in vehicles without filtering or using an unsuitable filter, otherwise, it will cause many troubles [2]. Harmful emissions lead to higher fuel consumption.

So, it requires to study the design factors of the pleated air filter influencing the performance characteristics of vehicle engines which directly affected by reducing the fuel consumption. R.J. Wakeman, et al. [3] simulated a model in permeable media and pleated filter cartridges. The effects of medium compression, pleat deformation, and pleat crowding were analyzed. The results were sensitive to the type and properties of the fluid being filtered, the properties of the filter medium, and the design configuration of the filter element. Zhang Mingxing, et al. [4] investigated the amounts of dust residual of a rectangular flat pleated filter during pulse cleaning. The results showed that when pulse interval or dust concentration was increased the dust residuals of the filter panel and the pressure drops of the filter were increased. Suresh Kalatoor, et al [5] Increased awareness of health effects caused by airborne contaminants that include natural and industrial aerosols, bioaerosols and gases, has led to increased usage of various kinds of filters.

Da-Ren Chen et al. [6] numerically optimized the pleated air filter using a steady laminar flow governed by the Darcy-Lapwood Brinkman. A dimensionless general correlation curve was predicted with different relevant parameters. Zhuangbo Feng and Zhengwei Long [7] simulated the unsteady filtration process in the pleated filter using both Lagrangian and Eulerian models. They found that the Eulerian model was faster than the Lagrangian method. Félicie Théron et al. [8] numerically and experimentally evaluated the influence of pleat geometrical characteristics on the performances of pleated fibrous filters in the depth filtration stage of submicronic aerosols. Andreas Wiegmann et al. [9] simulated the effect of pleat shape and filter media on the pressure drop by using the software tools PleatDict and ParPac. They showed how the capabilities of those codes can be extended by coupling them with the software tools GeoDict, FilterDict, and SuFiS. R.B. Simmons and S.A. Crow [10] utilized new and used cellulosic air filters for HVAC systems in vessels with a range of relative humidities (55-99%). J. T. Hanley et al. [11] evaluated the filtration efficiency of ventilation air cleaners over the 0.01 to 3 μm diameter size range. Results showed that efficiency was highly dependent on particle size, flow rate, and dust load present on the air cleaner. Rivers and Murphy [12] investigated 31 different air filters both clean and after clogging. Their study highlighted the dependence of the filter's resistance on the air velocity. K., Sutherland [13] presented the variation of pressure restriction of the filter based on time. N. Hasolli et al. [14] experimentally tested two models of two and three layers of filter media. The purpose is to obtain the optimum value of some filtration parameters. They found that the overall filtration performance was strongly dependent on the final layer that contributes to the dust-holding of the filter media. Laurent Oxarango et al. [15] analyzed a solution of the Navier-Stokes equation to determine the fluid flow in a two-dimensional porous channel with wall suction or injection as infiltration media. P.P. Bakane et al. [16] manifested the influence of dust particles through the air filter and its impact on the performance of the IC engines. The results presented that the fuel economy of modern gasoline vehicles was unaffected by filter clogging due to the closed-loop control and throttled operation of these engines. U. Stahl and H. Reinhardt [17] determined the increase of the pressure drop based on the exploitation time. Two types of air filters for the same engine were tested: the classic paper filter and the filter with progressive structure of nonwoven fibers. After 1,500 hours, the filters showed an increase of 2.5 kPa. The filters with progressive structure of nonwoven fiber showed an increase of the resistance of 2.5 kPa only after 3,500 hours. M. A. Barris [18] estimated the pleated air filter collection of dust. Under normal operating conditions, the filters that fit vehicle engines collected up to 2 g of dust for 1,600 km traveled. R. Yerrum et al. [19] in this paper, focus is given on optimizing the geometry of an intake system in automobile industry to reduce the pressure drop and enhance the filter utilization area. Based on existing model CFD results, geometrical changes like baffle placement in inlet plenum of the filter, inclusion of bell mouth in outlet plenum and dirty pipe, optimization of mesh size, removal of contraction in clean pipe of the intake system, etc. are carried out, to improve the flow characteristics. Park et al. [20] designed multiple types of pleated filter cartridges by changing pleat angle, pleat length, and number of pleats to get an optimum pleat ratio and found that the highest cleaning efficiency and best cleaning interval were achieved under the pleat ratio of 1.48. However, the pressure drop across the filter was found to be increased when the pleat ratio exceeded 1.48. Wakeman et al. [21] found that the filter media folds can reduce the permeability and cause losses of the effective filtration area due to media compression, pleat deformation, and pleat crowding. H. Kim et al. [22] A pleated filter can capture particulate matter, but the pressure loss across the filter medium is high compared to the electrostatic precipitator.

From previous literature, up to the author knowledge, there was no attempt to study the fuel consumption rate with different filter geometries. In this work, the performance characteristics of the pleated air filter associated with diesel engine are experimentally and numerically investigated. The effect of the different design parameters is discussed.

2. EXPERIMENTAL APPARATUS AND PROCEDURES

2.1. Experimental Set-Up

The experimental set-up is conducted through two steps which the pleated air filter is investigated as;

A. The filter specimens are tested in a pilot wind tunnel.
B. The filter specimens are associated with the I.C engine.

Figure 1 illustrated a photo of the wind tunnel in which the tested pleated air filter is incorporated (standard filter, loaded filter, and optimum filter) and associated with the measuring devices. The objective is

to measure the pressure drop across the pleated air filter for various air velocity.

FIGURE 1. A Photo of the test rig

The transparent wind tunnel consists of a rectangle duct of 0.185 m width, 0.260 m height, and 3 m length equipped with a discharge air blower with a centrifugal fan. The fan motor has a power 1HP and it is linked with a controlled regulator having a capability to fine-tuning the air velocity. The air velocity in the test section is changed from 1 m/s to 5 m/s. The pleated air filter is installed in the test section of the wind tunnel through a crossflow. Three filters (a, b, and c) are investigated at various air velocity as seen in Fig. 2, the details of the tested pleated air filters are given in Table 1.

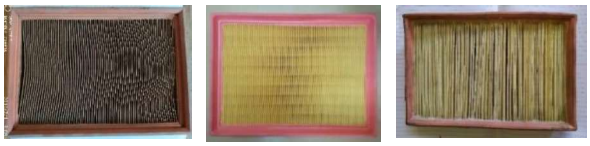

a. Loaded air filter b. Standard air filter c. Optimized air filter

FIGURE 2. Photos of the pleated air filters under investigation

TABLE 1. Dimensions of the pleated air filters

Filter media	Pleat length, (mm)	Pleat spacing, (mm)
Loaded filter	50	1
Standard filter	50	1
Optimized filter	25	1.4

Three pleated air filters are tested experimentally with the IC engine. The objective is to compute fuel consumption using the three filters. Fig. 3 shows a schematic diagram of the IC engine system used in the experiments.

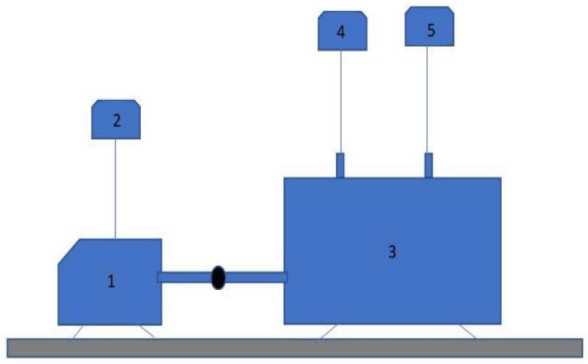

1-Dynamometer. 2-Torque meter. 3-I.C. engine. 4-Filter housing. 5-Fuel tank.

FIGURE 3. A schematic diagram of the IC engine system

The IC engine system consists of; a Ford XLD 1800 CC engine. Diesel engine with direct fuel injection is used to test the filters. The engine is conducted using hydraulic dynamometer with a maximum speed of 4800 rev/min. Table 2. Shows the internal combustion diesel engine specifications.

TABLE 2. Internal combustion engine specifications

Item	Specification
Power maximum, H.P.	60
Maximum speed, RPM	4800
Stroke, mm	82
Aspiration	Natural
No. of cylinders	4

2.2 MEASURING TECHNIQUES

The pressure drop across the pleated air filter is measured by a differential pressure model (Honeywell-DPTM100D) with an accuracy of ±0.1%. The velocity profile of the air through the duct section is identified according to ASHRAE recommendations [23] by hot-wire anemometer model (TM-4001) with an accuracy of ±0.01%. Twenty-Five grid points are fixed on the flow stream of the air duct to get the average air velocity. The engine rotational speed (RPM) is measured by infra-red laser tachometer model (DT6234B) with accuracy of 0.05% while the torque is measured by the torque meter associated with the dynamometer model (ET-DHA-1) with an accuracy of 1.0%.

3. NUMERICAL MODELING

The airflow characteristics are governed by the mass and momentum equation. In general, the governing equation can be formulated as, [3]:

$$\rho \frac{\partial \bar{\phi}}{\partial t} + \rho \bar{u}_j \frac{\partial \bar{\phi}}{\partial x_j} - \frac{\partial}{\partial x_j}\left[\Gamma_{eff} \frac{\partial \bar{\phi}}{\partial x_j}\right] = S_\phi \quad (1)$$

Where ϕ is the conserved quantity, Γ_{eff} the effective spread coefficient, S_ϕ the source term, and u_j the air velocity in the j direction, ρ the density of air.

In order to apply the governing equation to solve the pleated air filter model, a finite volume discretization method using a SIMPLEC-based solution algorithm of the velocity-pressure coupling is identified with a segregated solver. A commercial code of FLUENT-14.5 is used to solve numerical modeling. By applying the k-ε RNG turbulence model to adjust the model to deal with the flow characteristics of the pleated air filter. The transport equations of the RNG k-ε model are addressed as:

$$\frac{\partial}{\partial t}(\rho k)+\frac{\partial}{\partial x_i}[\rho k u_i]=\frac{\partial}{\partial x_j}\left[\alpha_k \mu_{eff}\frac{\partial k}{\partial x_j}\right]+G_k+G_b-\rho\varepsilon+S_k \quad (2)$$

$$\frac{\partial}{\partial t}(\rho\varepsilon)+\frac{\partial}{\partial x_i}(\rho\varepsilon u_i)=\frac{\partial}{\partial x_j}\left[\alpha_\varepsilon \mu_{eff}\frac{\partial \varepsilon}{\partial x_j}\right]+C_{1\varepsilon}\frac{\varepsilon}{k}(G_k+C_{3\varepsilon}G_b)-C_{2\varepsilon}\rho\frac{\varepsilon^2}{k}-R_\varepsilon+S_k \quad (3)$$

Where; $G_k=-\rho\overline{u_i'u_j'}\frac{\partial u_j}{\partial x_i}$,

$$R_\varepsilon=\frac{C_\mu\rho\xi^3(1-\xi/\xi_0)}{1+\psi\xi^3}\frac{\varepsilon^2}{k},$$

$$G_b=g_i\frac{\mu_t}{\rho Pr_t}\frac{\partial\rho}{\partial x_i}, C_{3\varepsilon}=\tanh\left|\frac{v}{u}\right|, S_k=\xi\varepsilon$$

The constants value; $C_{1\varepsilon}$, $C_{2\varepsilon}$, α_k, α_ε, ξ_0 and ψ in equations (2) and (3) are estimated as:

$C_{1\varepsilon}=1.42$; $C_{2\varepsilon}=1.68$; $\alpha_k=\alpha_\varepsilon\approx1.393$; $\xi=4.34$; and $\psi=0.012$; [24]

The term G_k represents the generation of turbulence kinetic energy due to the mean velocity gradients and G_b represents the generation of turbulence kinetic energy due to buoyancy.

The model domain is discretized into a group of control volumes. The governing equations of the model can be performed in a general form of a general variable, φ as:

$$\int_{CV}\frac{\partial(\rho\varphi)}{\partial t}+\int_{CV} div\,(\rho\varphi u)=\int_{CV} div\,(\Gamma\, grad\,\varphi)+\int_{CV} S_\varphi \quad (4)$$

A proper solution with the acclimatized grid elaboration of pending nodes technique (18800 nodes) is adopted, therefore, get the more economical use of grid nodes. The convergence criterion is particularized to be 10^{-6}. The boundary condition of the numerical model solution is approached at the upstream boundary that located; a uniform airflow with a velocity u_j is adjusted. At the downstream of the pleated air filter, the pressure is set to zero. Fig. 4 shows the grid cell number versus the pressure drop at a certain velocity of 3 m/s. It is noticed that refinement following a mesh size of 0.0001x0.0001 m^2 the pressure drop does not change as the mesh size changes and a mesh with this size is preferred for computation.

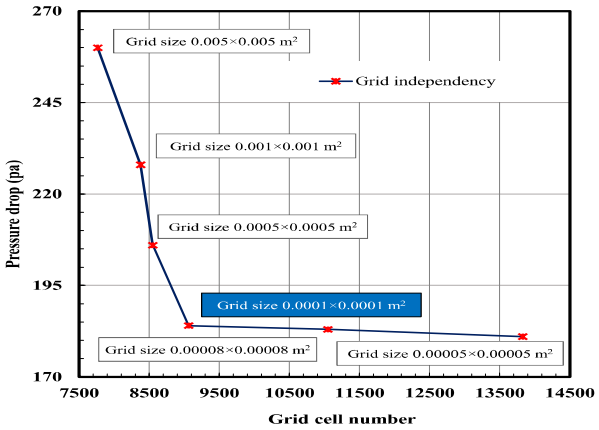

FIGURE 4. Numerical results of pressure drop for different grid cell system

The filter medium model is described as a porous cell media, which solves the momentum equation augmented by a general momentum form as:

$$\Delta p=-\frac{\mu}{k}v-C\frac{1}{2}\rho|v|v \quad (5)$$

Where the k and C are the permeability and the inertial factor of the porous medium respectively. A polynomial equation with conditions second order and zero constant term are applied to estimate the empirical constants as depicted in Fig.5. The filter correlation is predicted from the curve fit as:

$$\Delta p=2.84313\,v^2+48.1559\,v \quad (6)$$

Which the empirical values of the constants k and C are found to be 2.9824x10^{-7} m^2 and 2.4028 m^{-1} respectively.

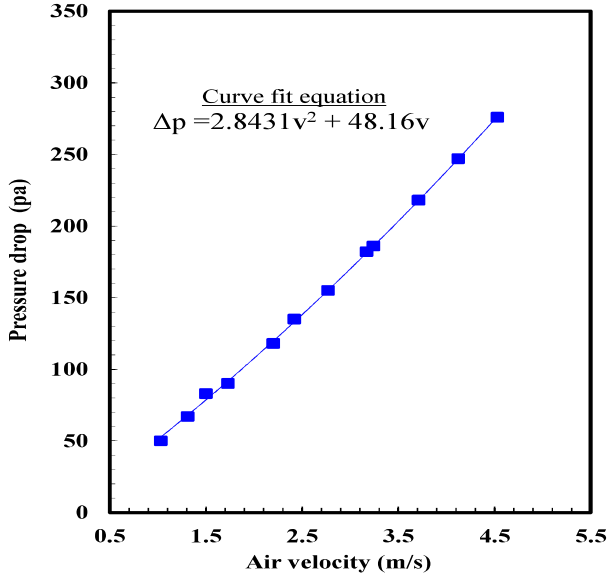

FIGURE 5. Curve fitting of the experimental data

Different pleated air filter models with design parameters are developed using commercial CFD-FLUENT 14.5 code. Table 3 illustrates the geometrical parameters of the pleated air filter.

TABLE 3. Geometrical parameters of the pleated air filter

Geometrical characteristics	Model specification					
Pleat length, L (mm)	25	45	50	55	60	—
Pleat height, H (mm)	0.40	0.45	0.50	0.55	0.60	0.70
Filter media thickness, δ (mm)	0.4	0.45	0.5	—	—	—

4. DATA REDUCTION

The engine brake power is calculated as follows:

$$BP = \frac{2\pi \cdot n \cdot T}{60} \quad (7)$$

The fuel mass flow rate is calculated as:

$$\dot{mf} = \frac{\rho v}{t} \quad (8)$$

The brake specific fuel consumption is calculated from the following equation:

$$BSFC = \frac{\dot{mf}}{BP} \quad (9)$$

5. Results and Discussion:

In this division, the performance characteristics of the pleated air filter associated with the I.C engine are experimentally and numerically investigated. Different parameters are investigated which are the validation of the present work, comparison between the loaded filter, the standard filter, and the optimum filter, effect of pleat length, effect of pleat height, effect of filter media thickness, and fuel consumption rate. The pressure drop of the pleated air filter for both experimental and computational results are illustrated in Fig. 6 for the same conditions in which the validation criteria is concerned. The results show that there is a good agreement between the experimental results and CFD predictions with a maximum error of 1.5%. The CFD numerical model of the pleated air filter is extended to cover more extra design and operational parameters.

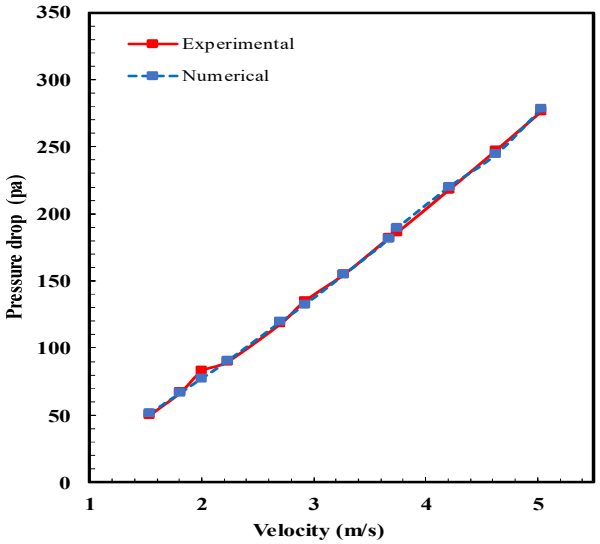

FIGURE 6. Validation of experimental data and numerical results

5.1 COMPARISON BETWEEN STANDARD, LOADED AND OPTIMIZED FILTER

Figure 7 shows a comparison between the pressure drop across the pleated air filter and the air average velocity for the optimized, standard and loaded filter. It can be observed from the figure that the pressure drop increases with the increases in air velocity for all types of filters. At a certain value of air velocity of 3.17 m/s, the pressure drop is 49, 182, 216 Pa for optimized, standard and loaded filter respectively. These results indicate that the pressure drop of loaded filter is higher than standard filter by 18.68% and also higher than optimized filter by 340.82%. The difference in the pressure drop between the standard filter and the loaded filter is referred to the effect of the amount of dust accumulated on the porous surface of the filter media in the loaded filter resulting an increase in the pressure drop whereas the variation in pressure drop between the optimized filter and the other filters is remarked due to the reducing of filter configurations.

5.2 Effect of the pleat length

Figure 8 shows the relation between the pressure drop and air velocity with different pleat lengths. It observed from the figure that, at a certain value of air velocity of 3.17 m/s, for L=55mm the pressure drop of the pleated air filter increased by 9.85%, for L=45mm the pressure drop decrease by 12.2%, for L=40mm the pressure drop decrease by 22.36, and for L=25mm the pressure drop decrease by 56.14% compared with the standard filter with L=50mm. Fig. 9a shows the contours of the velocity magnitude of the pleated air filter to appraise the effect of pleat length on the filter pressure drop at constant pleat height H=0.5 mm and the filter media thickness δ= 0.5 mm. The difference can be clearly seen at the entrance of the upstream channel where the air is separated, while a small fraction passes through the filter media. It has been remarked that the velocity increases at the inner of the upstream channel due to a decrease of the cross-sectional area due to the discharge speed and it is decreased by increasing the pleat length. Fig. 9b shows the pressure contours of the variation of pleat lengths at a constant height H=0.5 mm and thickness δ= 0.5 mm. It can be seen from the figure that the gradient in the pressure at the inner of the pleat where the pressure at the highest value at the inner as a result of the resistance of air filter media for the airflow and then the pressure gradually decreases.

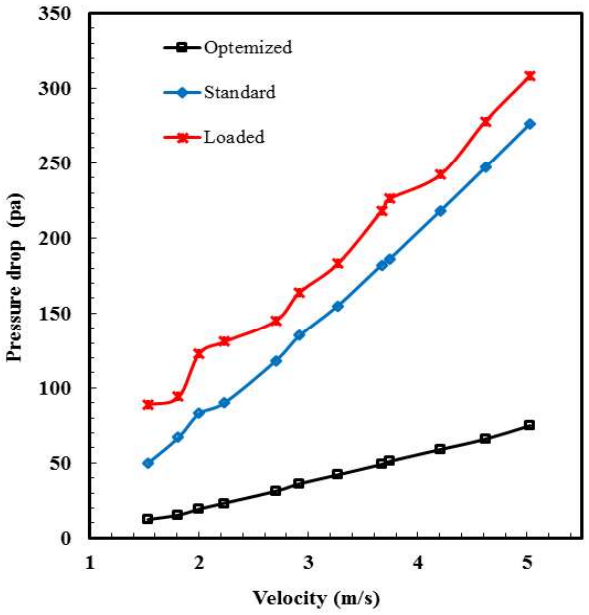

FIGURE 7. Pressure drop versus air velocity for different filter types as; optimized, standard and loaded

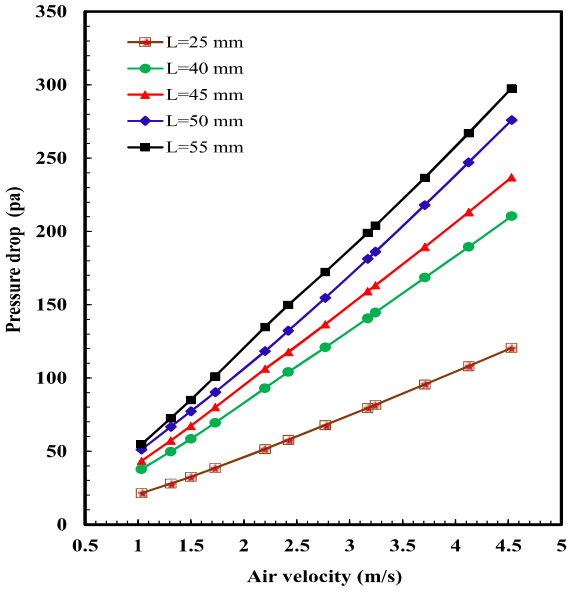

FIGURE 8. Variation of pressure drop versus air velocity with different pleat lengths

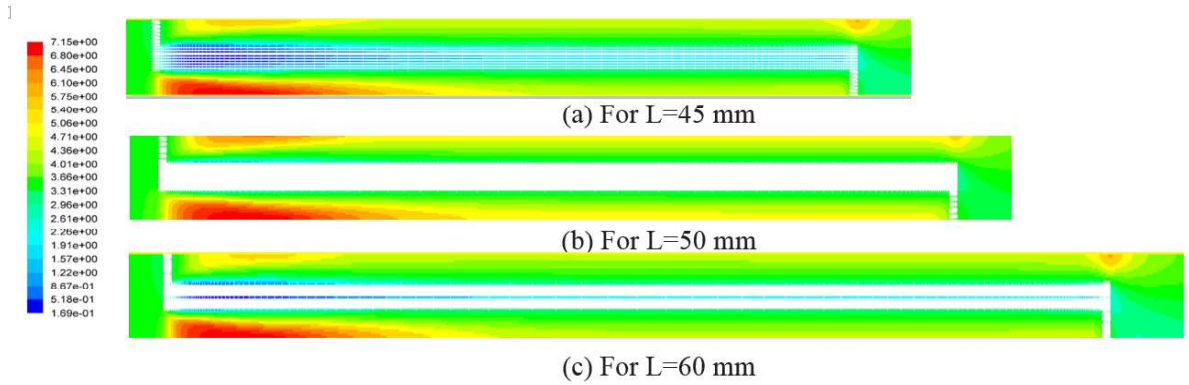

FIGURE 9a. Velocity magnitude for different pleat lengths of the pleated air filters at (a) L=45 mm, (b) L=50 mm, (c) L=60 mm.

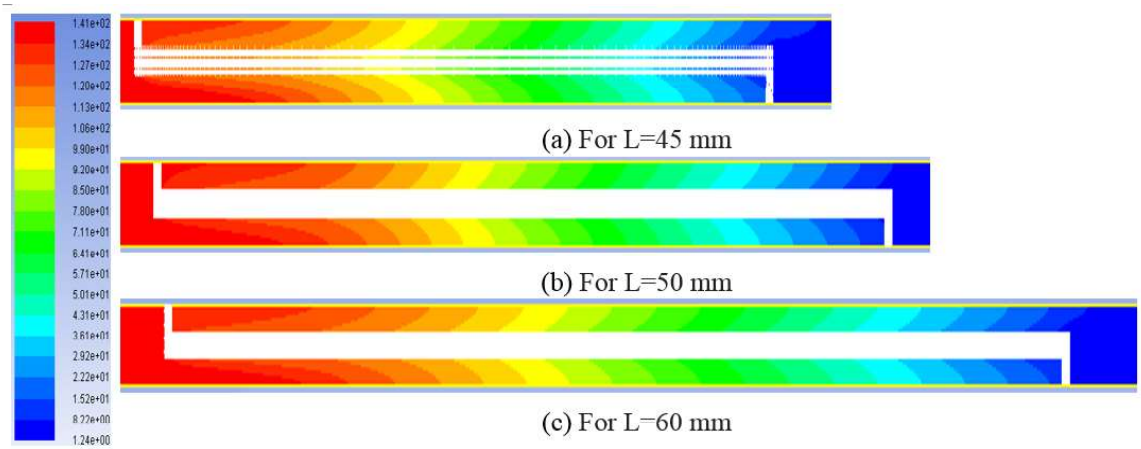

FIGURE 9b. Pressure contours of the pleated air filter for different pleat lengths at: (a) L=45 mm, (b) L=50 mm, (c) L=60 mm

5.3 EFFECT OF THE PLEAT MEDIA THICKNESS

Figure 10 shows the pressure drop comparison for different filter media thickness. It observed from the figure that the pressure drop increase by increasing the filter media thickness. At a certain velocity of 3.17 m/s at thickness of 0.45, the pressure drop is less than the standard filter by 4.59% and at the thickness of 0.40, the pressure drop is less than the standard filter by 9.4%. Fig. 11 shows the velocity magnitude of the filter media thickness. It observed from the figures that, the fraction passes through the filter media to the downstream channel is increased due to decrease in the filter media thickness and increase in the pleat height. At a small thickness and high height, the airflow through the filter media to the downstream channel is higher than the other cases due to decrease in the filter resistance as shown at height of 0.7mm and thickness of 0.4mm.

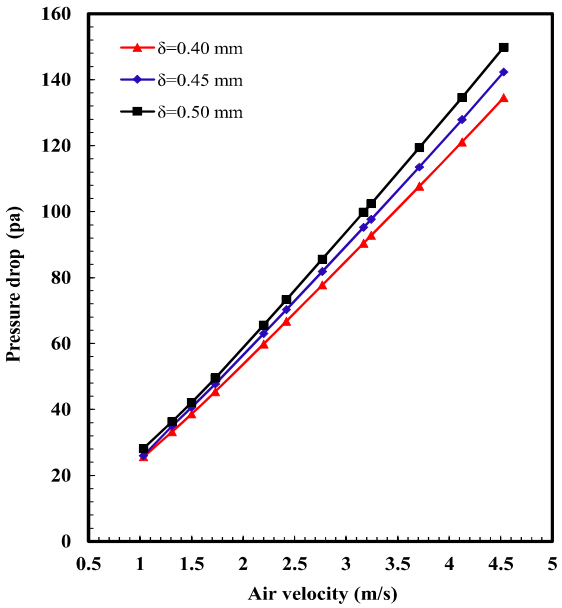

FIGURE 10. Variation of pressure drop versus air velocity with different pleat thickness

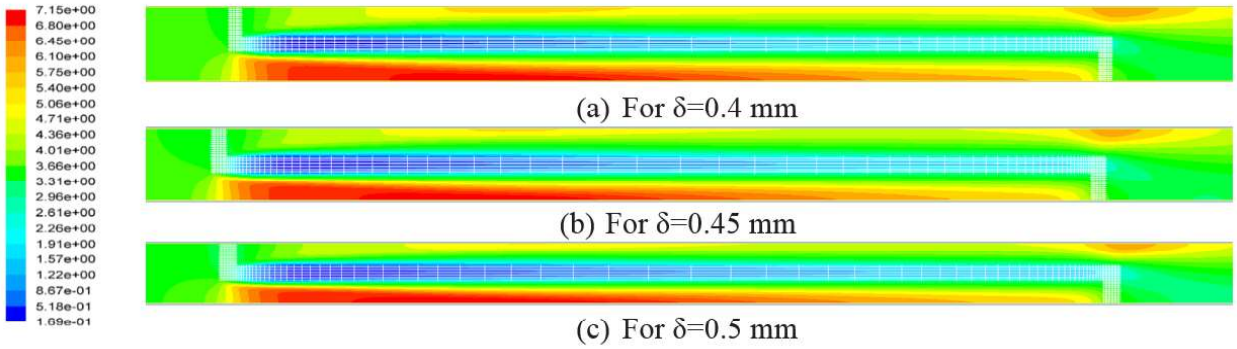

FIGURE 11. Effect of filter media thickness on the velocity magnitude: (a) at δ=0.4, (b) at δ=0.45, and (c) at δ=0.5 mm.

5.4 EFFECT OF THE PLEAT HEIGHT

Figure 12 shows a pressure drop comparison between different cases with different pleat height at constant pleat length and pleat media thickness. It can be seen from the figure that the less pressure drop is found with a pleat height of H=0.70 mm. At a certain value of air velocity of 3.17 m/s the pressure drop decrease by 30.87% about the standard filter and the pressure drop increase due to decrease in the pleat height. The contours of velocity magnitude and pressure are illustrated in Figs 13 and 14, respectively. It is seen from the figures that the pressure drop is increased with the decreasing the pleat height due to the separation of the flow stream.

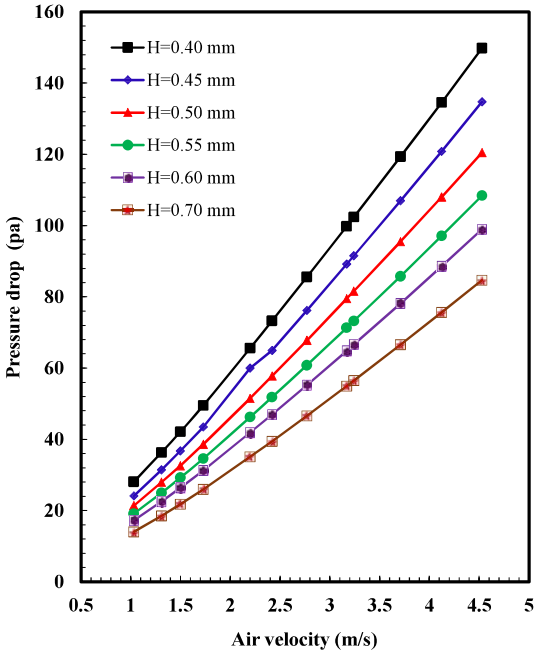

FIGURE 12. Variation of pressure drop versus air velocity with different pleat height.

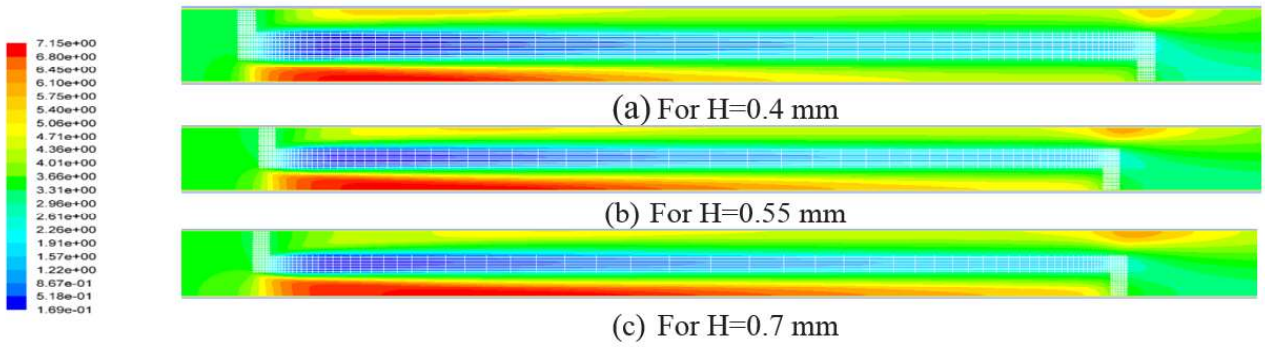

FIGURE 13. Effect of the pleat height on the velocity magnitude: (a) at H=0.4, (b) at H=0.55 and (c) at H=0.7 mm.

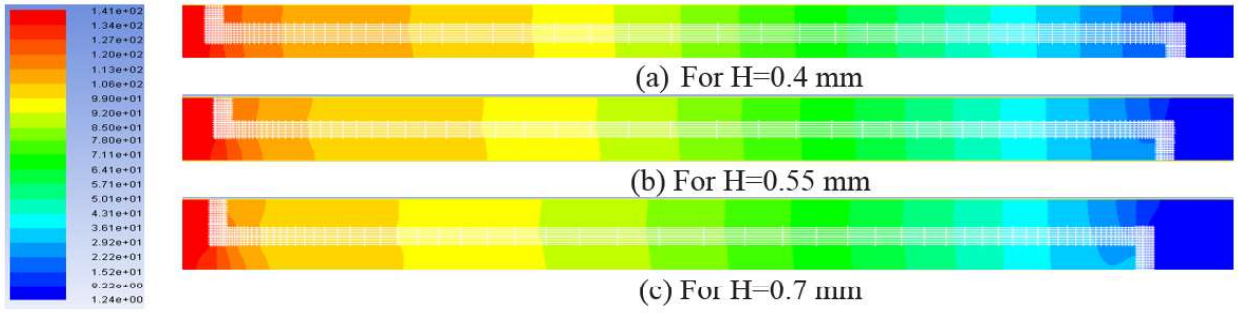

FIGURE 14. Effect of the pleat height on the pressure: (a) at H=0.4, (b) at H=0.55, (c) at H=0.7 mm.

5.5 INTERNAL COMBUSTION ENGINE FUEL SAVING

Figure 15 shows the engine brake specific fuel consumption versus engine speed at constant torque 197 N.m for the optimized, standard and loaded filter. It is clear that the optimum filter gives the lower fuel consumption and the loaded filter causes higher fuel consumption. At a certain value of engine speed of 1000 rpm, the fuel consumption of the engine when using the optimized filter was less than by 7.6 % when using the standard filter and by 34.38% when using the loaded filter due to the lower pressure drop for the optimized filter where the engine provides the amount of air needed for combustion without significant high loss. Fig. 16 shows the engine brake specific fuel consumption versus maximum torque for different engine speed. It can be seen from the figure that the optimized filter is the lower fuel consumption than the standard and the loaded filter for all values.

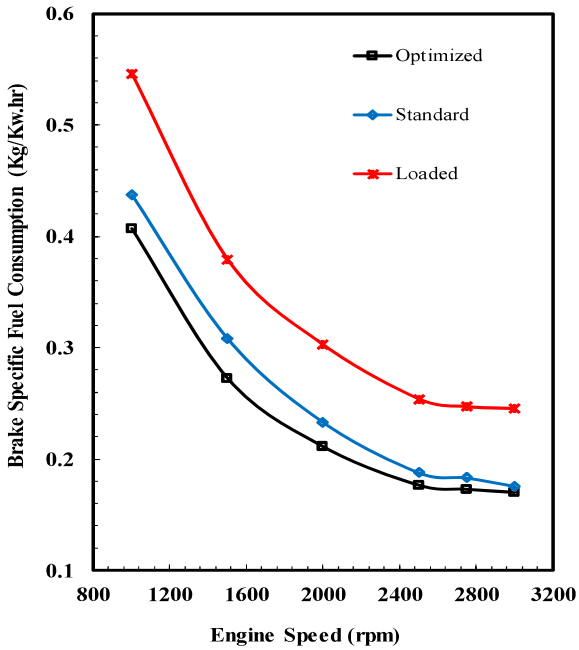

FIGURE 15. Engine brake specific fuel consumption vs. engine speed at constant torque (197 N.m).

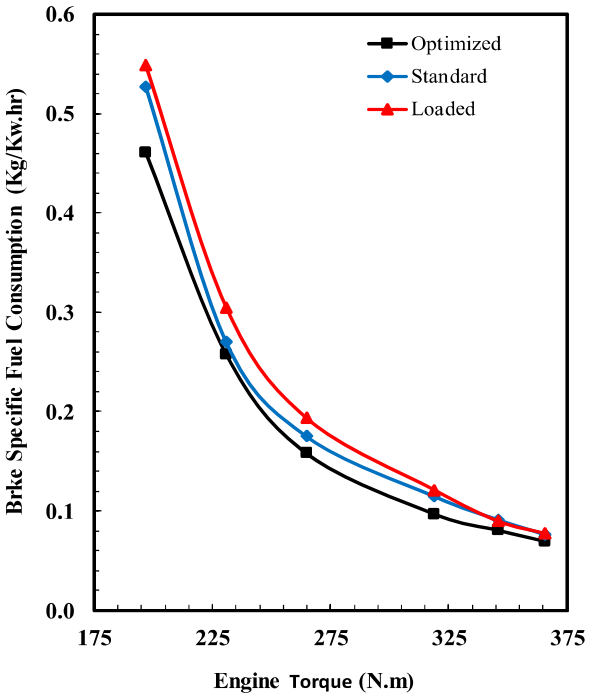

FIGURE 16. Engine brake specific fuel consumption vs. maximum torque for each engine speed.

6. CONCLUSIONS

In the present paper, the influence of various design factors (pleat length, pleat height, the thickness of filter media and fuel consumption rate) on the performance of the air filter was studied. Three pleated air filters were considered which are, the standard filter, the loaded filter, and the optimized filter. The conclusions are summarized as follows:

1. The optimized pleated air filter provided a lower consumption rate in comparing with loaded and standard filters by about 34.38 and 7.6%, respectively.
2. The increasing of the pleat length increases the pressure drop of the pleated air filter.
3. The increasing of the pleat height decreases the pressure drop of the pleated air filter.
4. The increasing of the pleat thickness increases the pressure drop of the pleated air filter.

REFERENCES

[1]. LDe Fabbroa, JC Labordeb, PMerlina, LRicciardib, "Air Flows and Pressure Drop Modelling for Different Pleated Industrial Filters", Filtration & Separation, 39 (2002) 34–40.

[2]. A. M. Saleh and H. Vahedi Tafreshi, "A simple semi-numerical model for designing pleated air filters under dust loading", Separation and Purification Technology, 137 (2014) 94–108.

[3]. R. J. Wakeman, N. S. Hanspal, A. N. Waghode and V. Nassehi, "Analysis of pleat crowding and medium compression in pleated cartridge filters". Chemical Engineering Research and Design, 83(2010) 1246–1255.

[4]. Zhang Mingxing, Chen Haiyan, Yan Cuiping, Li Qianqian, Qiu Jie, "Investigation to rectangular flat pleated filter for collecting corn straw particles during pulse cleaning", Advanced Powder Technology, 29 (2018) 1787-1794.

[5]. Kalatoor, Suresh; Legare, Pierre; Smith, Simon. "Filtration Efficiency of Automotive Cabin Air Filter Media Subjected to Different Aerosols under Various Environmental Conditions", SAE Technical Paper, 1997.

[6]. D. R. Chen, D. Y. H. Pui, and B. Y. H. Liu, "Optimization of pleated filter designs using a finite-element numerical model", Aerosol Science and Technology, 23 (1995) 579–590.

[7]. Z. Feng and Z. Long, "Modeling unsteady filtration performance of pleated filter, Aerosol Science and Technology", 50 (2016) 626–637.

[8]. F. Théron, A. Joubert, and L. Le Coq, "Numerical and experimental investigations of the influence of the pleat geometry on the pressure drop and velocity field of a pleated fibrous filter", Separation and Purification Technology, 182 (2017) 69–77.

[9]. A. Wiegmann, S. Rief, and D. Kehrwald, "Computational study of pressure drop dependence on pleat shape and filter media", pp. 1–8.

[10]. S. Immons, R.B. Crow, S.A. Fungal, "Colonization of air filters for use in heating, ventilating, and air conditioning (HVAC) systems". Journal of industrial microbiology, (1995) 14.1: 41-45.

[11]. J. T. Hanley, D.S. Ensor, D.D. Smith, L.E. Sparks, "Fractional aerosol filtration efficiency of in-duct ventilation air cleaners", Indoor Air, 4.3 (1994): 169-178.

[12]. D.R Rivers, D.J. Murphy, "Air filter performance under variable air volume conditions", ASHRAE Transactions, 106 (2000)131-144.

[13]. K. Sutherland, "Filters and filtration handbook, third ed", Elsevier, Oxford (2008) 27-40.

[14]. N. Hasolli, Y. O. Park, and Y. W. Rhee, "Experimental study on filtration performance of flat sheet multiple-layer depth filter media for intake air filtration", Aerosol Science and Technology, 47 (2013) 1334–1341.

[15]. L. Oxarango, P. Schmitz, and M. Quintard, "Laminar flow in channels with wall suction or injection: A new model to study multi-channel filtration systems", Chemical Engineering Science, 59 (2004) 1039–1051.

[16]. P. P. Bakane, Y. Burghate, V. Pathe, and S. Fulzele, "Review on Air Filter Cleaning Machine for Automobile", vol. 2, no. 2, pp. 1–8.

[17]. U. Stahl, H. Reinhardt, "New nonwoven media for engine intake air filtration with improved performances", SAE technical paper series, (2006) 01-0272.

[18]. M.A. Barris, "The influence of filter selection on engine wear, emissions, and performance", SAE technical paper series, (1995) 952557

[19]. Yerram, Ravinder, et al, "Optimization of Intake System and Filter of an Automobile using CFD analysis", Quality Engineering & Software Technologies (QUEST), Bangalore, (2006).

[20]. B.H. Park, M.H. Lee, Y.M. Jo, S.B. Kim, "Influence of pleat geometry on filter cleaning in a PTFE/glass composite filter", J. Air Waste Manage. Assoc. 62 (2012) 1257-1263.
[21]. R.J. Wakeman, N.S. Hanspal, A.N. Waghode, V. Nassehi, "Analysis of pleat crowding and medium compression in pleated cartridge filters", Chem. Eng. Res. Des, 83 (2005)1246-1255.
[22]. H. Kim, Han B., Kim, Y., Oda, T., and Won, H. (2013). "Submicrometer Particle Removal Indoors by a Novel Electrostatic Precipitator with High Clean Air Delivery Rate, Low Ozone Emissions, and Carbon Fiber Ionizer", Indoor Air, 23:369-378.
[23]. "ASHRAE handbook of fundamentals. SI edition", chapter 14, ASHRAE Inc., Atlanta, GA, USA; 2001
[24]. Fluent Inc., FLUENT, user's manual, USA, 2005.